



Uncertainty budgets of major ozone absorption cross-sections used in UV remote sensing applications

Mark Weber¹, Victor Gorshchev¹, and Anna Serdyuchenko^{1*}

¹Institut für Umweltphysik, Universität Bremen FB1, PO Box 330 440, D-28334 Bremen, Germany

5 *now at: OHB System AG, Manfred-Fuchs-Straße 1, D-82234 Weßling, Germany

Correspondence to: Mark Weber (weber@uni-bremen.de)

Abstract. Detailed uncertainty budgets of three major UV ozone absorption cross-section datasets that are used in remote sensing application are provided and discussed. The datasets are Bass-Paur (BP), Brion-Daumont-Maliget (BDM), and the more recent Serdyuchenko-Gorshchev (SG). For most remote sensing application the temperature dependence of the Huggins
10 ozone band is described by a quadratic polynomial in temperature (Bass-Paur parameterisation) by applying a regression to the cross-section data measured at selected atmospherically relevant temperatures. For traceability of atmospheric ozone measurements uncertainties from the laboratory measurements as well as from the temperature parameterisation of the ozone cross-section data are needed as an input to detailed uncertainty calculation of atmospheric ozone measurements. In this
15 paper the uncertainty budgets of the three major ozone cross-section datasets are summarised from the original literature. The quadratic temperature dependence of the cross-section datasets is investigated. Combined uncertainty budgets is provided for all data sets based upon Monte Carlo simulation that includes uncertainties from the laboratory measurements as well as uncertainties from the temperature parameterisation. Between 300 and 330 nm both BDM and SG have an overall uncertainty of 1.5%, while BP has a somewhat larger uncertainty of 2.1%. At temperatures below about 215 K, uncertainties in the BDM data increase more strongly than the others due to the lack of very low temperature laboratory measurements
20 (lowest temperature of BDM available is 218 K).

1 Introduction

The three ozone absorption cross-sections in common use for many remote sensing applications are the Bass Paur (BP) data (Bass and Paur 1985; Paur and Bass, 1985), the Daumont-Brion-Maliget (BDM) data (Daumont et al., 1992; Brion et al., 1993; Maliget et al., 1995) and the very recent Serdyuchenko-Gorshchev (SG) data (Gorshchev et al., 2014; Serdyuchenko et
25 al., 2011; 2014). While the data from BDM and SG are absolute cross-section measurements, the BP data were scaled to the so-called Hearn value at the Hg line wavelength (253.65 nm). The standard retrievals applied to the ground Brewer and Dobson spectrophotometer data use the BP data (e.g. Redondas et al., 2014), while the satellite community uses any of the three data sets or other data (WMO-GAW, 2015; ACSO, 2010; Orphal et al., Absorption cross-sections of ozone - Status report 2015, manuscript in preparation).



30 For the review of uncertainties, original publications reporting on results of the experimental work were considered first. Since BP data was absolutely scaled using Hearn data (Hearn, 1961), the latter is also included in this review. There is a lack of consistency in the presentation of measurement uncertainty budgets across different papers. Neither of the publications uses the guidelines and recommended definitions as outlined in JCGM-100 (2008). An attempt to analyze and harmonize the reported uncertainties is made in the following sections. In some cases not all measured quantities were reported and in most cases detailed description of the data processing procedures is missing. It is very likely that the published measurement uncertainties are incomplete and the overall uncertainties thus underestimated.

35 In this paper we start with a brief summary on measurement principles in the laboratory (Section 2), followed by a review of the uncertainties of the UV ozone cross-section data (Section 3). In Section 4 the temperature dependence in the three major ozone cross-section datasets are discussed followed by Section 5, which summarises the Monte-Carlo simulation to obtain the overall uncertainty budgets of the major datasets. Section 6 provides a summary and conclusion.

2 Measurement technique

Ozone absorption cross-sections are produced by performing spectroscopic measurements and subsequent analysis to convert the recorded spectra into absorption cross-sections in units of $cm^2/molecule$. The absorption spectroscopy is based on the Beer-Lambert law, which describes the attenuation of the light intensity transmitted through the absorbing medium.

45 For gaseous species the Beer-Lambert law can be written as:

$$I(\lambda) = I_0(\lambda) \int_0^L e^{-n(T,p,\ell) \cdot \sigma(\lambda,T)} d\ell. \quad (1)$$

Here $I_0(\lambda)$ is the light intensity in the absence of absorbing molecules (background), n is the absorbing gas number density, which is generally a function of temperature T , pressure p , and the position ℓ along the beam path, L is the total absorption path length and σ [$cm^2/molecule$] is the wavelength-dependent (and normally also temperature-dependent) absorption cross-section.

50 In a laboratory environment it is possible to control the experimental conditions with sufficient precision, so that the number density n [cm^{-3}] is assumed to be homogeneously distributed along the absorption path of a known length L [cm]. From measurements of other parameters, such as T [K] and p [Pa], the value of n is calculated assuming the ideal gas law ($p = n \cdot k_B \cdot T$, k_B Boltzmann constant). In this case Eq. 1 can be transformed to:

$$A(\lambda, T) = 1 - I/I_0 = 1 - \exp[-\sigma(\lambda, T) \cdot n \cdot L], \quad (2)$$

where A is the unitless absorbance. The unitless optical density (OD) is then expressed as

$$OD(\lambda, T) = \ln(I/I_0) = \sigma(\lambda, T) \cdot n \cdot L. \quad (3)$$



55 Absolute cross-sections can be derived from the optical density if species concentration, temperature and absorption path length are known. Since ozone is a reactive and highly explosive gas, many measurements were done using a flow of oxygen/ozone mixture, where the partial pressure of ozone is unknown and values from other published absolute ozone cross-section measurements are used to find a scaling factor that converts the measured optical density into absorption cross-section (e.g. Chegade et al., 2013a, b)

60 Alternatively, measurements performed at selected wavelengths with a special attention to control of the experimental parameters are used to calibrate the relative cross-sections (optical densities). The latter was done for the BP data (Bass and Paur 1985, Paur and Bass, 1985) as all their relative spectra were scaled to the ozone absorption cross-section value at 253.65 nm (mercury line) as reported by Hearn (1961). Thus the uncertainties in the reference data propagate into the calibrated spectra.

65 Depending on the kind of spectrometer used for broadband (Fourier transform, grating) or single wavelength measurements, registered spectra are inevitably subject to multiple *sources of uncertainties* - stochastic intensity variations caused by detector noise, light source intensity fluctuations etc. (JCGM-100, 2008). Spectral *random error* can be characterized by the signal-to-noise ratio (*SNR*), and one of the ways to improve the quality of the measurements is acquisition of multiple spectra obtained under *repeatable conditions* (JCGM-100, 2008). Uncertainty of the resulting average
70 value is represented by the standard deviation of the mean.

Spectrometers are characterized by the spectral resolution and wavelength calibration to some reference values, which influences the wavelength uncertainty of the produced data. For example, dispersion-based instruments can be wavelength-calibrated using isolated atomic emission lines of Hg or Cd lamps, and Fourier-transform spectrometers are auto-calibrated with the built-in stabilized He-Ne laser.

75 Instrumental uncertainties of other measured quantities - temperature T , ozone (partial) pressure p , absorption path length L are also contributing to the total absorption cross-section uncertainty. For broadband laboratory measurements covering a large wavelength range, like the Hartley-Huggins band of ozone, cross-section values change by up to seven orders of magnitude, so that optical density spectra are recorded using different combination of cell lengths and partial pressures (e.g. Gorshelev et al. 2014, Serdyuchenko et al. 2014). The various spectra are then concatenated to cover the entire spectral
80 range, which leads to additional uncertainties.

3 Review of reported uncertainties

3.1 Uncertainty budget of Hearn

Dating back to 1961, Hearn reported on ozone absorption cross-sections at six selected wavelengths, of which the value at $\lambda = 253.65$ nm is of particular interest, since it has been measured in many studies and is considered a standard reference
85 (see Viallon et al. (2015) and references therein). The following information of the laboratory measurements by Hearn (1961)



are known:

- spectral resolution: 0.09 nm (Hg emission line width at 253.65 nm)
- temperature: 295 K
- temperature uncertainty: not reported (“Errors due to the variation of the temperature of the ozone-oxygen mixture during the experiment are quite negligible. The apparatus was housed in a cellar, the temperature of which was thermostatically controlled.”)
- Absolute scaling: pressure observation of the pure O₃ → O₂ decomposition

90

95

Table 1 provides the original notation of uncertainty budget from Hearn (1961). The uncertainties are divided into type A and type B uncertainties (JCGM-100, 2008). Type A uncertainty means that it is derived from a statistical analysis and an observed frequency distribution. Type B uncertainties are not derived from a statistical analysis and it assumes a probability distribution that is based upon past experiences or is derived from external specifications. The breakdown of evaluation type of the uncertainties is color coded in Table 1.

Table 1: Summary of uncertainties as reported by Hearn (1961). Light gray highlighting stands for type A, dark gray for type B uncertainties.

| “Random errors” | | | | |
|--|---|------------------------------|----------|----------------|
| Wavelength uncertainty at 253.65 nm | RMS deviation (mean of 6 observations) | Absorption length (0.744 cm) | Pressure | Total SD (RMS) |
| 0.09 nm | 1.05 % | 0.54 % | 0.81 % | 1.4 % |
| Type B | Type A | Type B | | |
| “Systematic errors” | | | | |
| Wavelength uncertainty at 253.65 nm | Correction for stray light | Correction for companion | | |
| 0.09 nm | 0.0 | - | | |
| “Best estimates of the absorption coefficients” | | | | |
| Wavelength uncertainty at 253.65 nm | Molecular absorption cross-section | | | |
| 0.09 nm | $114.7 \pm 2.4 \cdot 10^{-19} \text{ cm}^2$ | | | |

100

105

Little to no detail is provided on the accuracy of the instruments used during measurements. Given the reported $\pm 2.4 \cdot 10^{19} \text{ cm}^2$ interval around the $114.7 \cdot 10^{-19} \text{ cm}^2$ value of absorption cross-section and assuming rectangular distribution of possible values (JCGM-100, 2008), the relative standard measurement uncertainty of the ozone absorption cross-section is estimated at 1.4%. Adding up all uncertainties the Hearn value has a precision of 2%. It should be noted here that more recent measurements (Viillon et al., 2015, Jansson C. et al., Absolute ozone absorption cross section at 253.65 nm revisited, manuscript in preparation) indicate lower values for the mercury line that lies about 1.4 to 1.8% lower than Hearn’s value, but it is within the uncertainty of the Hearn’s experiment. Compared to all available measurements reported, Hearn’s value is close to the upper range of values (e.g. Sofen et al., 2015, WMO-GAW, 2015),



3.2 Uncertainty budget of BP

110 The team of Bass and Paur (Bass and Paur 1985, Paur and Bass, 1985) provided cross-section data for a broad spectral range and at several temperatures. The following information is available from the BP data:

- Wavelength range: 245 – 343 nm
- Spectral resolution: 0.025 nm
- Wavelength grid: 0.05 nm
- 115 — Wavelength calibration: 23 points between 200 and 365 nm (Hg, Cd, Zn lines)
- Temperatures: 203 K, 218 K, 228 K, 243 K, 273 K, 298 K

Table 2 summarises the uncertainties of BP data, with a type A/B breakdown color-coded in different gray shadings. The relative standard measurement uncertainty of the BP ozone absorption cross-section is stated to be around $\pm 1\%$. It seems to be an underestimation, since BP relative spectra were scaled to the Hearn value at 253.65 nm, which is reported with a 1.4% relative standard measurement uncertainty (see Section 3.1).

120

Table 2: Absolute uncertainties reported by Bass and Paur (1985) and Paur and Bass (1985). Light gray highlighting stands for type A , dark gray for type B uncertainties.

| Uncertainty | Values |
|--|---|
| Wavelength uncertainty | 0.025 nm |
| Uncertainty in the transmittance determination | 2 in 105 (arising from counting statistics) |
| Sample temperature stability | better than 1 K |
| Temperature uncertainty | 0.25 K |
| Pressure measurement uncertainty | 1 mbar |
| Absolute scaling | using the value of Hearn at 253.65 nm |

125

3.3 Uncertainty budget of BDM

Ozone absorption cross-sections provided by Brion et al. (1993), Daumont et al. (1992) and Malicet et al. (1995) further extend the wavelength coverage (into the visible) compared to BP. The following information is available on the experimental details for BDM data in the Hartley-Huggins ozone absorption band:

- 130 — Wavelength range: 195 – 345 nm (except at 273 K: 300–345 nm)
- Spectral resolution: 0.01 nm
- Wavelength grid: in steps of 0.01 nm
- Concatenation: 15 nm wide spectral cuts, 5 nm overlap
- Number of spectra averaged: 10
- 135 — Temperatures: 218 K, 228 K, 243 K, 273 K, 295 K
- Temperature uncertainty: from 0.05 K @ 295 K to 0.3 K @ 218 K



- Light source reference spectra: recorded before and after the ozone spectra
- Absolute scaling: measurements of total pressure

140 Table 3 provides the original notation of the uncertainty budget of BDM data with Type A / Type B breakdown color-coded in gray shadings. The information on the relative standard measurement uncertainty of the BDM ozone absorption cross-section is wavelength-dependent (see last row of Table 3).

Table 3: Summary of uncertainties as reported by Brion et al. (1993), Daumont et al. (1992) and Malicet et al. (1995). Light gray highlighting stands for type A, dark gray for type B uncertainties.

145

| Quantity | Uncertainty |
|------------------------|--|
| Optical density | 1 % (for $\lambda < 335$ nm) |
| Optical path | 0.05 % |
| Ozone pressure | 0.1 % |
| Impurities | < 0.1 % |
| Temperature | from 0.02 % @ 295 K up to 0.15 % @ 218 K |
| Wavelength | < 0.05 % (Hartley band 200 – 280 nm) < 0.8 % (Huggins band 280 – 340 nm) |
| Total systematic error | 1.3 – 1.5 % (Hartley band 200 – 280 nm) 1.3 – 3.5 % (Huggins band 280 – 340 nm) |
| Random error RMS | 0.3 – 2.2 % (for $\lambda < 340$ nm) |

3.4 Uncertainty budget of SG

Ozone absorption cross-sections reported by Serdyuchenko et al. (2014) were obtained for 11 temperatures in a wide spectral range using two spectrometers (Fourier-transform and Echelle-grating spectrometers). Tables 4 and 5 summarize the information on the experimental details and uncertainties for the SG cross-section data.

150 In the 213-350 nm wavelength region the relative standard measurement uncertainty of the SG ozone absorption cross-section is wavelength-dependent and ranges between 1 – 3 %. The dominating uncertainty source is the statistical repeatability of the spectral registration, influenced by stability of the light source and detector noise. These two factors have a greater impact when the intensities of the spectra contributing to the OD calculation either differ greatly (strong absorption, close to saturation) or are very close to each other. This effect is demonstrated in Figure 1, showing the concatenated OD spectrum and relative uncertainties of the corresponding constituent spectral cuts. The latter were calculated according to law of propagation of uncertainty using standard deviation (variances) and mean values of I and I₀ spectra which determine the optical density OD (see Eq. 3).

Table 6 summarises the uncertainties for all cross-sections datasets discussed here.

160



Table 4. Experimental details and statistical uncertainty of OD spectra for different wavelength regions for SG data (Serdyuchenko et al., 2014).

| Region, [nm] | Spectrometer, detector | Resolution [nm] | Calibration | Path, [cm] | Lamp stability* [%] | Optical density |
|--------------|------------------------|-----------------|-------------|------------|----------------------|-----------------|
| 213 – 310 | Echelle, ICCD | 0.018 | Relative | 5 | D ₂ , 0.5 | 0.5 – 2 |
| 310 – 335 | FTS, GaP | 0.01 | Absolute | 135 | Xe, 2 | 0.1 – 2 |
| 335 – 350 | FTS, GaP | 0.012 | Relative | 270 | Xe, 1 | 0.1 – 1 |
| 350 – 450 | Echelle, ICCD | 0.02 | Relative | ~2000 | Xe, 1 | 0.05 – 1 |
| 450 – 780 | FTS, Si | 0.02-0.06 | Absolute | 270 | W, 0.2 | 0.05 – 2 |
| 780 -1100 | FTS, Si | 0.12-0.24 | Relative | 270 | W, 0.2 | 0.001 – 0.1 |

* during the entire measurement

D₂, Xe - deuterium and xenon discharge lamps, W - tungsten filament lamp

165

170

Table 5. Summary of absolute and relative measurement uncertainties for SG dataset. Light gray highlighting stands for type A, dark gray for type B uncertainties.

| Systematic uncertainty (abs) | (rel) [%] | Statistical uncertainty (abs) | (rel) [%] |
|---|-------------|---|-----------|
| Ozone impurity: | 0.005 | Ozone initial pressure | < 1 |
| oxygen impurity leaks | < 0.1 | Pressure fluctuations (< 0.04 mb) | < 0.08 |
| Pressure sensors (0.02 mb) | 0.04 | Temperature fluctuations (<0.3 K) | < 0.1 |
| Temp. sensors offset (1 K) | 0.3 – 0.5 | Light source stability, relative to optical density OD = 1 (depending on spectral region) | 0.2 – 2 |
| Temp. non-uniformity (1 K) | 0.3 – 0.5 | | |
| Cell length (0.1-1.0 mm) | 0.04 – 0.07 | | |
| Combined standard relative uncertainty (excluding low absorption regions near 380nm and above 800nm) | | | |
| | 0.4 – 0.7 | | 1 – 2.2 |

175



Table 6. Uncertainties for Hearn, BP, BDM and SG ozone cross-sections.

| Dataset | Scaling method | Type A (Statistical) | Type B | Relative standard measurement uncertainty, [%] |
|-------------------|----------------------|-------------------------|--------------------------------------|--|
| Hearn (253.65 nm) | Absolute, pure ozone | 1.05 | – | 1.4 |
| BP | Using Hearn | 1 | 2.1 | > 2.1 |
| BDM | Absolute, pure ozone | 0.9 - 2.2 | 1.3 (Hartley) 1.3 - 3.5 (Huggins) | 2 - 3 2 - 4 |
| SG | Absolute, pure ozone | 1 - 2.2 | 0.4 - 1.7 | 1.1 - 3 |

180

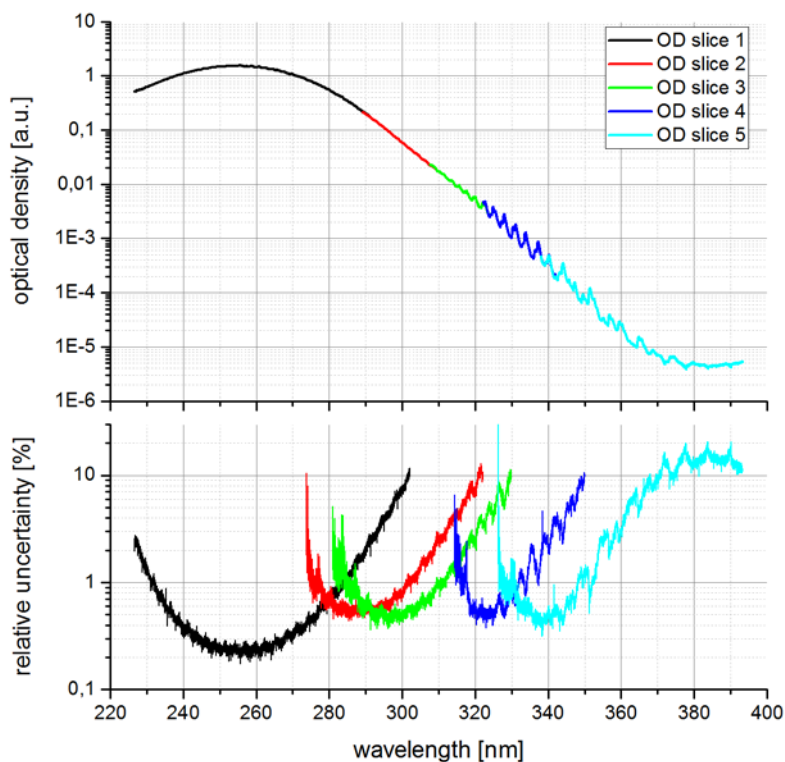


Figure 1. Upper panel: concatenated optical density spectrum. Lower panel: relative uncertainty of various OD spectra used for concatenation. Instruments: Echelle/FTS; number of averaged spectra: 2000 (Echelle)/100 (FTS); acquisition time: ~ 30 minutes; light sources: Xe and D₂ lamps. From Serdyuchenko et al. (2014).



4 Temperature dependence and uncertainties

In general the ozone cross-sections were determined at selected atmospherically relevant temperatures. BP and BDM data encompass six and five temperatures, respectively, while SG is available at eleven temperatures. The original data can be obtained from http://satellite.mpic.de/spectral_atlas/cross_sections/Ozone/O3.spc. Table 7 summarises the available temperatures for all three datasets.

Table 7. Available temperatures for various ozone absorption cross-section data. Temperatures provided in brackets were not used to determine temperature coefficients since they did not cover the complete wavelength range of 290-340 nm.

| Ozone absorption cross-section | Temperatures [K] | Wavelength range [nm] |
|--------------------------------|---|-----------------------|
| BP (Paur & Bass, 1985) | 203, 218, (228), 243, 273, 298 | 245 - 343 |
| BDM (Malicet et al., 1995) | 218, 228, 243, (273), 295 | 195 - 345 |
| SG (Serdyuchenko et al., 2014) | 193, 203, 213, 223, 233, 243, 253, 263, 273, 283, 293 | 213 - 1100 |

190

The temperature dependence of the ozone absorption cross-sections is commonly described by the so-called Bass-Paur parameterisation (Paur and Bass, 1985), which is a quadratic polynomial:

$$\sigma_p(\lambda, t) = a_0(\lambda) + a_1(\lambda)t + a_2(\lambda)t^2. \quad (4)$$

The temperature coefficients a_0 , a_1 , a_2 are determined in a multivariate linear regression using the cross-section data $\sigma(\lambda, t_i)$ measured at various temperatures t_i . They were calculated in the wavelength range 290-360 nm (BP: up to about 338 nm), which is the spectral range with the highest temperature sensitivity (Huggins ozone band). The temperature t in Eq. 4 is given in degree Celsius ($t=T-273.15$ K). The uncertainty of the calculated cross-section at a given temperature is then given by

$$\Delta\sigma_p = \sqrt{(\Delta a_0)^2 + (\Delta a_1)^2 t^2 + (\Delta a_2)^2 t^4}. \quad (5)$$

The 228 K temperature data of BP has been excluded from the polynomial fit as there is a gap between 295 and 304 nm. Liu et al. (2007) noted a systematic bias in the 273 K BDM data and reported better ozone retrieval fit results if this temperature is excluded. This temperature data also does not provide data below 300 nm. As noted by Orphal and Chance (2003) and Weber et al. (2013), there is a systematic wavelength shift between BP and BDM. Shifting the BP data by +0.029 nm leads to better agreement (to within 0.5%) between BDM and BP (Weber et al., 2013). The SG data wavelength scale agrees to within uncertainties with BDM (Gorshelev et al., 2014).



Figures 2 to 4 show the temperature coefficients including the 1-sigma uncertainties (see Eq. 5) for the BP, BDM, and
205 SG data, respectively. As the SG data are somewhat noisy near 300 nm, in the July 2013 version of the SG data a fast
Fourier transform filter was applied in the spectral range 213-317 nm.

Figure 5 shows the uncertainty from the polynomial fit as a function of wavelength for T=193 K and 227 K. BP data
uncertainties are getting fairly large above 330 nm reaching nearly 25% for some wavelengths at 220 K and more than 60%
210 at 193 K. The uncertainty of the BDM data ranges between 0 and 2% up to 330 nm, while SG data show a fairly constant
uncertainty of about 1% on average at T=227 K. The uncertainties are doubled at the lower temperature. The very low
uncertainty for BP and BDM at some wavelength is mainly due to the very low number of available temperatures (4-5) that
leads in some cases to overfitting of the data with a quadratic polynomial.

The spectral resolution of the three datasets varies from 0.01 nm (BDM) to 0.05 nm (BP). The instrumental slit function
215 can be easily applied to each of the temperature coefficients in order to match the spectral resolution of the cross-section data
in form of Eq. 4 to any type of instruments.

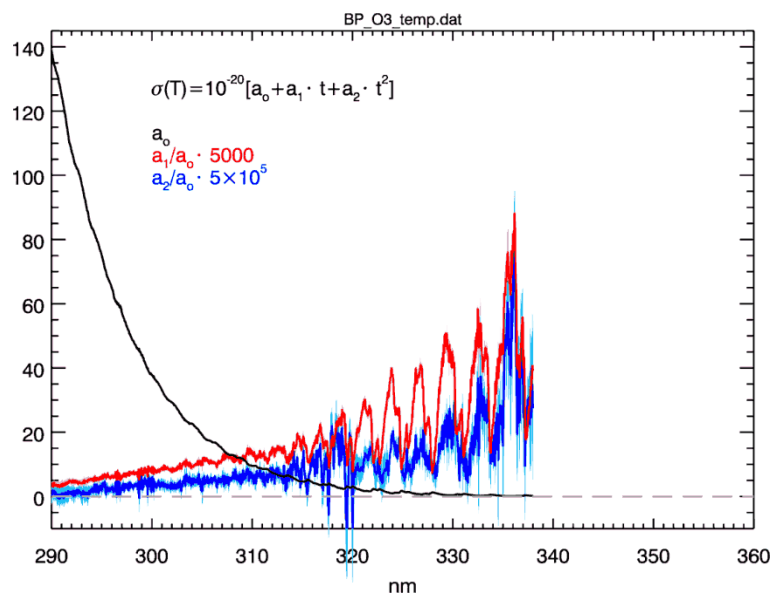


Figure 2. Temperature coefficients and their uncertainty (1-sigma) of the BP data.

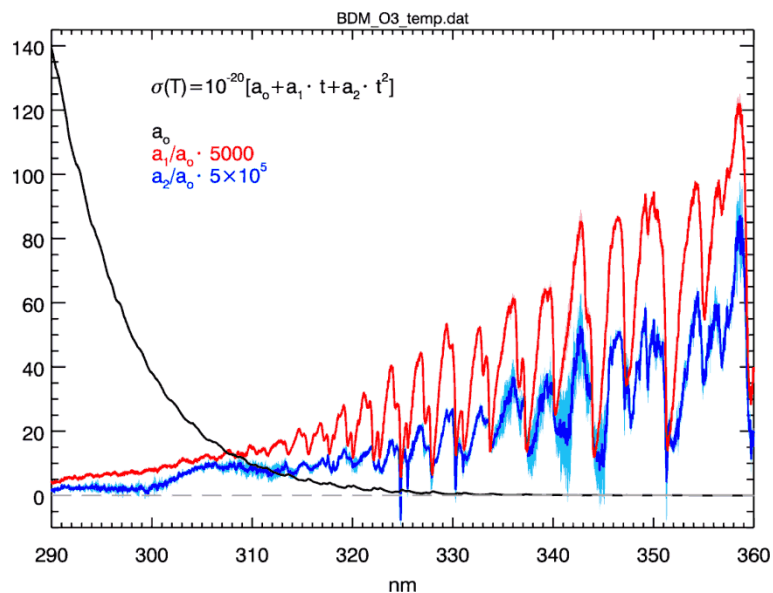


Figure 3. Same as Fig. 2, but for BDM data.

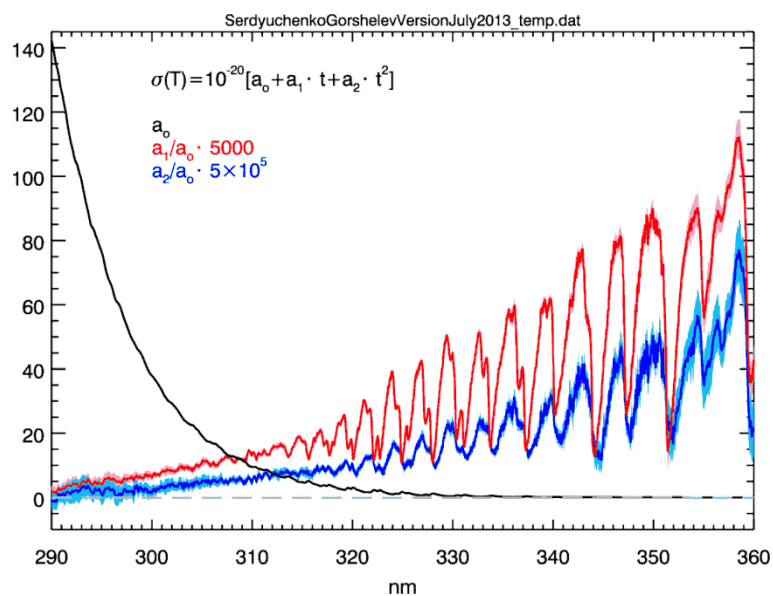


Figure 4. Same as Fig. 2, but for SG (July 2013 version) data.

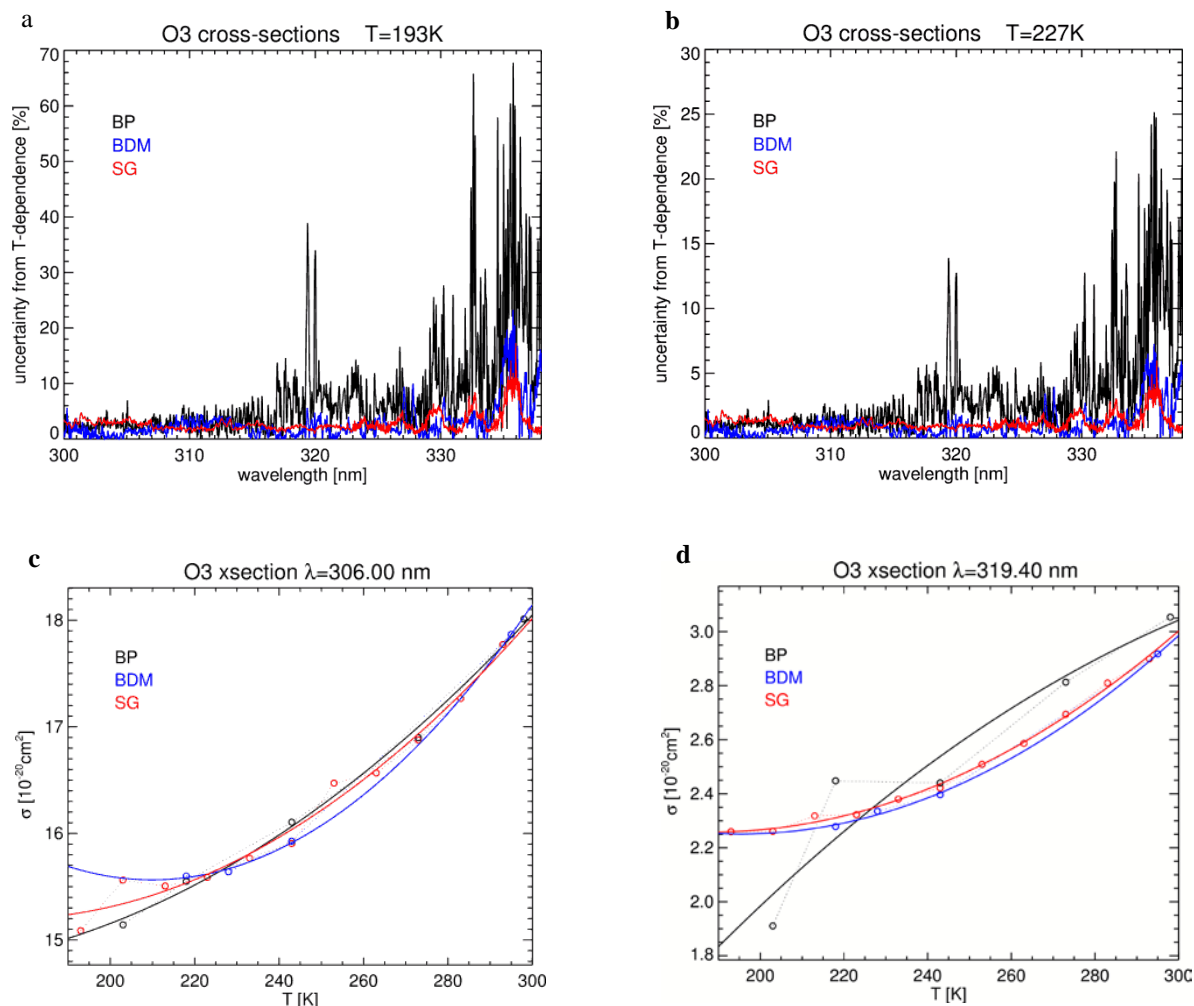


Figure 5. Panels a and b: 1-sigma uncertainty of BP, BDM, and SG ozone cross-sections at T=193 K and 227 K, respectively, from the polynomial temperature fit (Eq. 5). Note the change in scale of the ordinate axes. Panels c and d: Measured ozone cross-sections (points) and polynomial fit (solid lines) for BP, BDM, and SG at 306 and 319.4 nm, respectively.

5 Overall uncertainty: Monte – Carlo simulation

The uncertainty given in Eq. 5 reflects only the uncertainty from the temperature parameterisation using a polynomial (if we assume that a quadratic dependence in temperature is true). In order to estimate the overall uncertainty including uncertainties from measurements (random and systematic), wavelength registration, and the temperature parameterisation, an

225 extensive Monte-Carlo simulation (JCGM-101, 2008) was carried out.



Table 8 summarises the uncertainties simulated. The numbers are mainly based upon the uncertainty as reported in Table 6. It was assumed that the probability density function (PDF) is Gaussian for all uncertainties.

Table 8. Uncertainties accounted for in the Monte-Carlo simulation.

230

| Uncertainty type (290 nm – 370 nm) | Value (1-sigma) |
|--|---|
| Measurement at each T (random) | 1% |
| Measurement at each T (systematic) | 1.3%* |
| Wavelength registration at each T (random) | 0.005 nm |
| Wavelength registration at each T (systematic) | 0 nm** |
| Temperature T (random) | 0.5 K |
| Temperature T (systematic) | 1 K |
| Polynomial in T | combined resampling residuals and wild boot strap (normal distributed) |

* 2% for BP ozone cross-sections

** it is assumed that wavelength shifts can be corrected in ozone retrievals (e.g. Coldewey-Egbers et al., 2015)

235 The values used here are the minimum uncertainties (see Table 6), however, it should be noted that the (random) measurement uncertainties varies with wavelengths, but this is neglected here. Random uncertainties are simulated by randomizing for each temperature data in a given simulation, while systematic errors means an uncertainty drawn from the random generator being applied to all the temperature data simultaneously.

In order to estimate the effect of the measurement errors on uncertainties from the T-polynomial a combination of the resampling residual and wild boot strap method was applied (Wu, 1986). The residual from the polynomial fit is given by

$$\epsilon_j = \sigma(\lambda, t_j) - \sigma_p(\lambda, t_j), \quad (6)$$

where $\sigma_p(\lambda, t_j)$ is the fitted polynomial (see Eq. 4). In the Monte Carlo simulation the residual is distributed randomly to different temperatures as follows

$$y(t_j) = \sigma(\lambda, t_j) + \zeta \epsilon_j \quad (7)$$

and the polynomial fit repeated. ζ is a normal distributed random number. The normally distributed random number generator used in the MC simulation is based upon the Box-Muller transform (Box and Muller 1958). The total sample size selected was 10^4 , which provided a reasonable compromise between computation time and precision of the simulation. For each wavelength between 290 and 370 nm (BP: ~339 nm) in steps of 0.01 nm the Monte-Carlo simulation was carried out.

245 Figures 6 and 7 show the results from the MC simulation of uncertainties for the three major ozone cross-section data at 319.4 nm and 306 nm, respectively, as an example. These plots are corresponding to the data shown in panels **c** and **d** of Figure 5. The uncertainties are very similar for BDM and SG, except for the lowest temperatures ($T < 215$ K) where BDM uncertainties increase due to the extrapolation of the fitted polynomial. The larger systematic measurement uncertainty of

250



the BP data (2%) leads to larger overall uncertainties in the BP data. At 319.4 nm there appears to be some issue, since the 203 K BP measurements are much lower than SG leading to rather large polynomial fit errors as observed earlier.

Figure 8 shows the uncertainties as a function of wavelengths for selected temperatures. At 227 K the overall uncertainties are about 1.5% for both BDM and SG, while BP uncertainties are about 2.1% (1-sigma). Above 330 nm the uncertainties increase for all datasets. At very low temperatures, e.g. 193 K, the BDM uncertainties increase to about 4% (1-sigma), while SG remains at 2% (1-sigma). BP uncertainties are about 2.5% (1-sigma) and are also lower than BDM. Similar to 227 K, the uncertainties increase at the longest wavelengths. At temperatures above 215 K, the uncertainties of BDM and SG are very similar, at lower temperatures the BDM uncertainties significantly increases due to the lack of very low temperature measurements.

260 6 Summary and conclusion

Realistic and comparable uncertainty budgets were derived from three major ozone absorption cross-section datasets that are used in various remote sensing applications. First a review of the published literature on the uncertainty of the BP, BDM, and SG datasets was given. The uncertainties of these three datasets are summarized in Table 6 and are now directly comparable between the various datasets. For remote sensing application, in particular in the Huggins ozone band, the temperature dependence of the ozone cross-sections have to be accounted for and this is typically done using a quadratic polynomial as a function of temperature. Using the updated uncertainty estimates from Table 6 and a residual boot strap method for estimating the uncertainties from the temperature polynomial, a Monte Carlo simulation was carried out. However, one should note that due to lack of information from the peer-review literature on the exact wavelength dependence of the uncertainties (see Table 6) this was neglected in our simulations.

In the Huggins band the overall uncertainty of the temperature dependent ozone cross-section is about 1.5% (1-sigma) for BDM and SG and 2.1% (1-sigma) for BP up to about 330 nm. At temperatures below about 215 K the uncertainty in the BDM data increase more strongly than for the others, as the lowest measured temperature for BDM is 218 K and the extrapolation of the polynomial leads to larger uncertainties. Above 330 nm the uncertainties increase significantly for all datasets. Ozone retrievals exploiting the UV spectral range usually focus on wavelengths below 335 nm.

The temperature coefficients for the three major cross-section data with uncertainty estimates from the polynomial fit alone as well as from the MC simulations are available at <http://www.iup.uni-bremen.de/~weber/ATMOZ>.



280

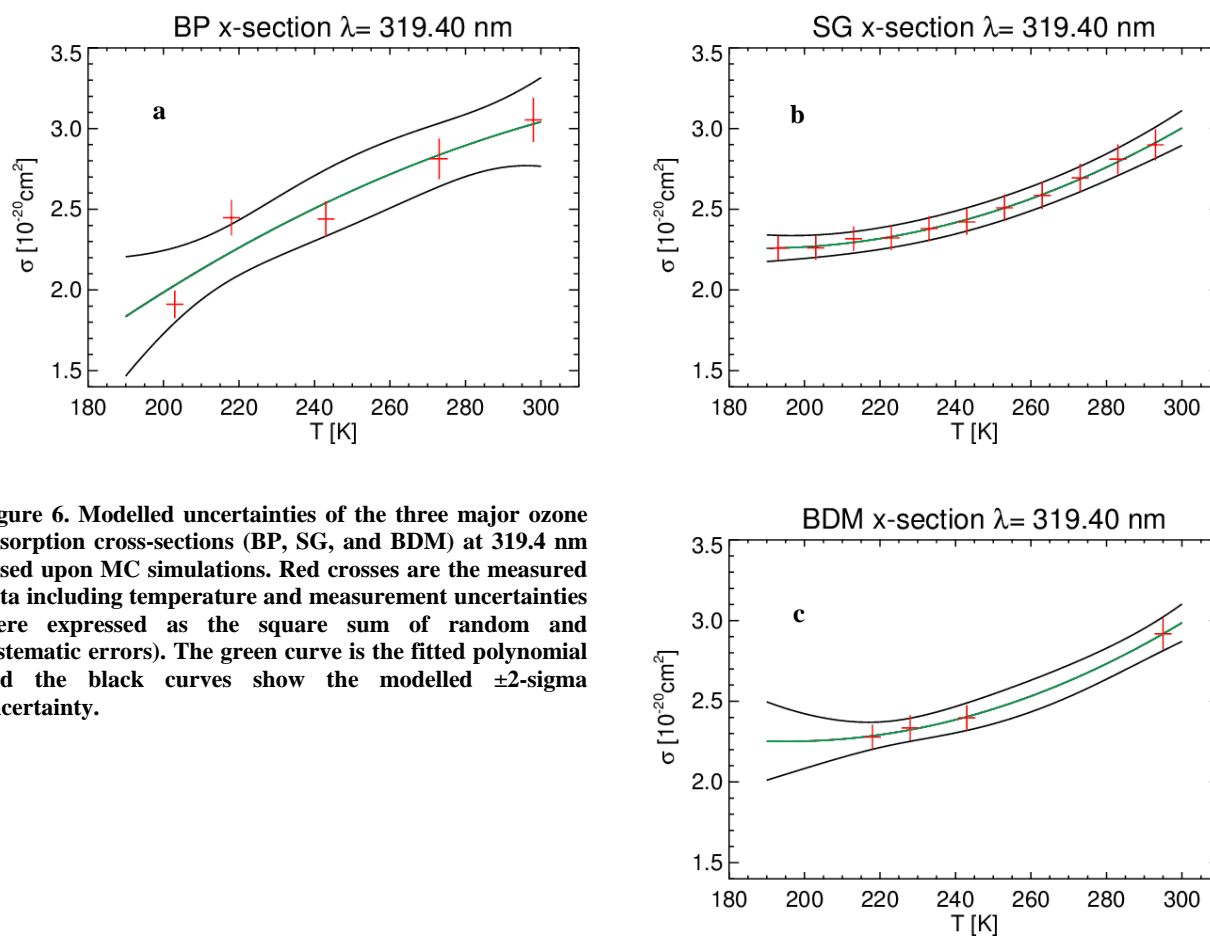


Figure 6. Modelled uncertainties of the three major ozone absorption cross-sections (BP, SG, and BDM) at 319.4 nm based upon MC simulations. Red crosses are the measured data including temperature and measurement uncertainties (here expressed as the square sum of random and systematic errors). The green curve is the fitted polynomial and the black curves show the modelled ± 2 -sigma uncertainty.

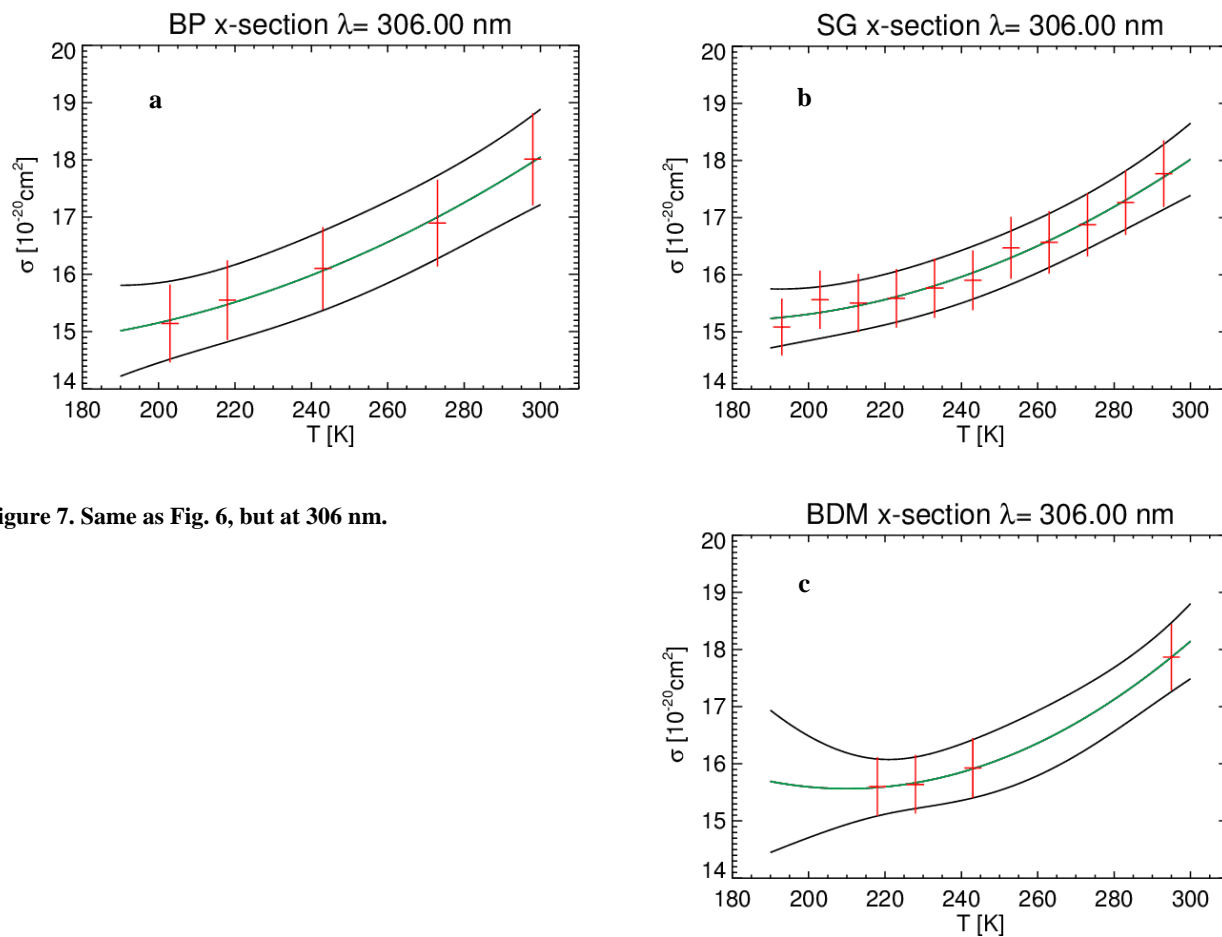


Figure 7. Same as Fig. 6, but at 306 nm.

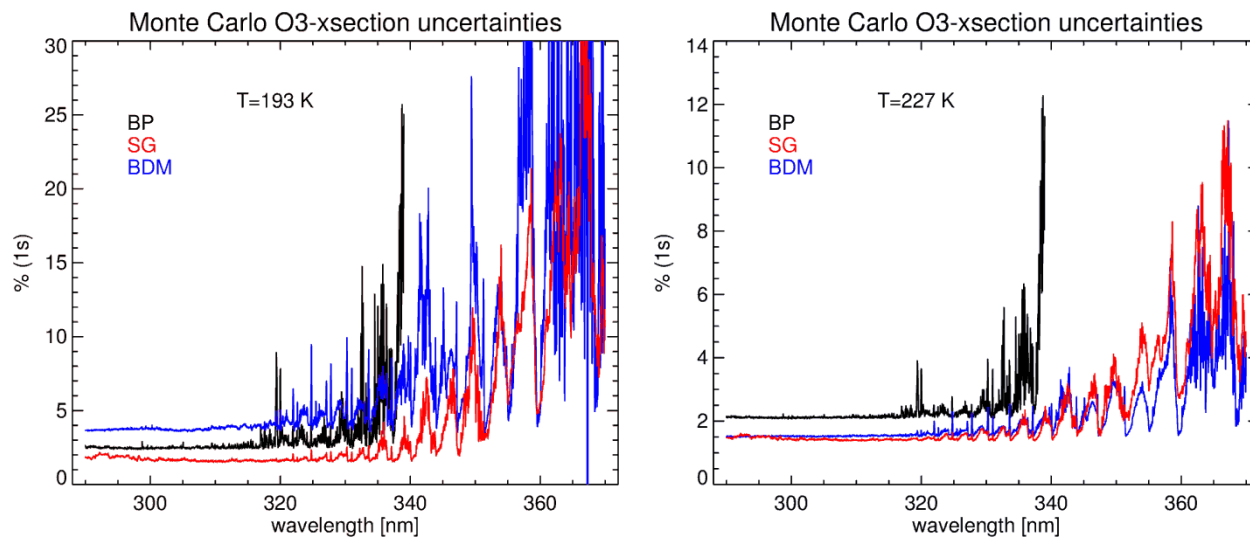


Figure 8. Uncertainty (1-sigma) of BP, BDM, and SG ozone cross-sections at T=193 K (left) and 227 K (right), respectively, from the MC simulation. Note the change in scale of the ordinate axes.

285

Acknowledgment

This work was supported in part by a grant from EMRP within the ENV59-ATMOZ (‘Traceability for Atmospheric Total Column Ozone’) Joint Research Programme (JRP), University of Bremen, and the State Bremen. The EMRP is jointly funded by the EMRP participating countries within EURAMET and the European Union.

290

References

ACSO: WMO/GAW-IO3C-IGACO-O3 Activity “Absorption Cross Sections of Ozone (ACSO)”, <http://igaco-o3.fmi.fi/ACSO/>, last accessed: November 2015, 2010.

Bass, A. M. and Paur, R. J.: The ultraviolet cross-sections of ozone: I. the measurements, in: Atmospheric Ozone, edited by: Zerefos, C. S. and Ghazi, A., Proc. Quadrennial Ozone Symposium, Halkidiki, Greece, 1984, Reidel, D., Dordrecht, 606–610, 1985.

Box, G. E. P. and Muller, M. E.: A note on the generation of random normal deviates. *Ann. Math. Stat.* 29, 610-611, 1958.



- Brion, J., Chakir, A., Daumont, D., Malicet, J. and Parrisé, C.: High-resolution laboratory absorption cross section of O₃. Temperature effect, *Chem. Phys. Lett.*, 213, 610–612, doi:10.1016/0009-2614(93)89169-I, 1993.
- 300 Chehade, W., Gür, B., Spietz, P., Gorshelev, V., Serdyuchenko, A., Burrows, J. P., and Weber, M.: Temperature dependent ozone absorption cross section spectra measured with the GOME-2 FM3 spectrometer and first application in satellite retrievals, *Atmos. Meas. Tech.*, 6, 1623-1632, doi:10.5194/amt-6-1623-2013, 2013.
- Chehade, W., Gorshelev, V., Serdyuchenko, A., Burrows, J. P., and Weber, M.: Revised temperature-dependent ozone absorption cross-section spectra (Bogumil et al.) measured with the SCIAMACHY satellite spectrometer, *Atmos. Meas. Tech.*, 6, 3055-3065, doi:10.5194/amt-6-3055-2013, 2013.
- 305 Coldewey-Egbers, M., Weber, M., Lamsal, L. N., de Beek, R., Buchwitz, M., Burrows, J. P.: Total ozone retrieval from GOME UV spectral data using the weighting function DOAS approach, *Atmos. Chem. Phys.* 5, 5015-5025, 2005.
- Daumont, D., Brion, J., Charbonnier, J. and Malicet, J.: Ozone UV spectroscopy I: Absorption cross-sections at room temperature, *J. Atmos. Chem.*, 15, 145–155, doi:10.1007/BF00053756, 1992.
- 310 Gorshelev, V., Serdyuchenko, A., Weber, M., and Burrows, J. P.: High spectral resolution ozone absorption cross-sections: Part I. Measurements, data analysis and comparison around 293K, *Atmos. Meas. Tech.*, 7, 609-624, doi:10.5194/amt-7-609-2014, 2014.
- JCGM-100: Evaluation of measurement data – Guide to the expression of uncertainty in measurement (JCGM-100), http://www.bipm.org/utis/common/documents/jcgm/JCGM_100_2008_E.pdf, last accessed: November 2015, 2008
- 315 JCGM-101: Evaluation of measurement data - Supplement 1 to the “Guide to the expression of uncertainty in measurement” - Propagation of distributions using a Monte Carlo method (JCGM-101), http://www.bipm.org/utis/common/documents/jcgm/JCGM_101_2008_E.pdf, last accessed: October 2015, 2008.
- Hearn, A. G.: The absorption of ozone in the ultra-violet and visible regions of the spectrum, *Proc. Phys. Soc.*, 78, 932–940, doi:10.1088/0370-1328/78/5/340, 1961.
- 320 Liu, X., Chance, K., Sioris, C. E. and Kurosu, T. P.: Impact of using different ozone cross sections on ozone profile retrievals from Global Ozone Monitoring Experiment (GOME) ultraviolet measurements, *Atmos. Chem. Phys.*, 7, 3571–3578, doi:10.5194/acp-7-3571-2007, 2007.
- Malicet, J., Daumont, D., Charbonnier, J., Parrisé, C., Chakir, A. and Brion, J.: Ozone UV spectroscopy. II. Absorption cross-sections and temperature dependence, *J. Atmos. Chem.*, 21, 263–273, doi:10.1007/BF00696758, 1995.



- 325 Park, S. K. and Miller, K. W.: Random number generators: good ones are hard to find, *Commun. ACM*, 31, 1192–1201, doi:10.1145/63039.63042, 1988.
- Paur, R. J. and Bass, A. M.: The ultraviolet cross-sections of ozone: II. Results and temperature dependence, in: *Atmospheric Ozone*, edited by: Zerefos, C. S. and Ghazi A., Proc. Quadrennial Ozone Symposium, Halkidiki, Greece, 1984, Reidel, D., Dordrecht, 611–615, 1985.
- 330 Redondas, A., Evans, R., Stuebi, R., Köhler, U., and Weber, M.: Evaluation of the use of five laboratory determined ozone absorption cross sections in brewer and dobson retrieval algorithms, *Atmos. Chem. Phys.*, 14, 1635–1648, doi:10.5194/acp-14-1635-2014, 2014.
- Serdyuchenko, A., Gorshelev, V., Weber, M., and Burrows, J. P.: New broadband high-resolution ozone absorption cross-sections, *Spectroscopy Europe*, 23, 14–17, 2011.
- 335 Serdyuchenko, A., Gorshelev, V., Weber, M., Chehade, W., and Burrows, J. P.: High spectral resolution ozone absorption cross-sections – Part 2: Temperature dependence, *Atmos. Meas. Tech.*, 7, 625–636, doi:10.5194/amt-7-625-2014, 2014.
- Sofen, E. D., Evans, M. J., and Lewis, A. C.: Updated ozone absorption cross section will reduce air quality compliance, *Atmos. Chem. Phys.*, 15, 13627–13632, doi:10.5194/acp-15-13627-2015, 2015.
- Viallon, J., Lee, S., Moussay, P., Tworek, K., Petersen, M., and Wielgosz, R. I.: Accurate measurements of ozone absorption cross-sections in the Hartley band, *Atmos. Meas. Tech.*, 8, 1245–1257, doi:10.5194/amt-8-1245-2015, 2015.
- Weber, M., Chehade, W., Gorshelev, V., Serdyuchenko, A., Spietz, P.: Impact of ozone cross-section choice on WFD OAS total ozone retrieval applied to GOME, SCIAMACHY, and GOME-2 (1995–present), Technical Note Issue 2 with updates from November 2013, a contribution to IGACO-O3/ACSO, 2013, http://www.iup.uni-bremen.de/UVSAT_material/technotes/weber_acso_201311.pdf, last accessed: November 2015, 2013.
- 345 WMO-GAW: Absorption Cross-Sections of Ozone (ACSO) Status Report June 2015, WMO-GAW Report 218, World Meteorological Organization, Geneva, Switzerland, http://www.wmo.int/pages/prog/arep/gaw/documents/FINAL_GAW_218.pdf, 2015.
- Wu, C. F. J.: Jackknife, bootstrap and other resampling methods in regression analysis (with discussions), *Ann. Stat.* 14, 1261–1350, doi:10.1214/aos/1176350142, 1986.